World Scientific
www.worldscientific.com

JAPAN SOCIETY OF CIVIL ENGINEERS
COASTAL ENGINEERING COMMITTEE

Coastal Engineering Journal, Vol. 48, No. 4 (2006) 309–336

POROUS EFFECT PARAMETER OF THIN PERMEABLE PLATES

YUCHENG LI*
State Key Laboratory of Coastal and Offshore Engineering, Dalian University of Technology, Dalian 116024, China
The R&D Center of Civil Engineering Technology, Dalian University, Dalian 116622, China
Tel: +86-411-84708974; Fax: +86-411-84708526
liyuch@dlut.edu.cn

YONG LIU
State Key Laboratory of Coastal and Offshore Engineering, Dalian University of Technology, Dalian 116024, China
lyong@student.dlut.edu.cn

BIN TENG
State Key Laboratory of Coastal and Offshore Engineering, Dalian University of Technology, Dalian 116024, China
bteng@dlut.edu.cn

Received 7 November 2005
Revised 19 June 2006

The present paper aims at getting the porous effect parameter G of a thin permeable wall. The reflection and transmission coefficients of a thin vertical porous wall with different porous shapes and porosities are obtained by a physical model experiment. The reflection coefficient and total horizontal wave load on a perforated caisson are also obtained by another experiment. Analytical solutions of wave interaction with these two vertical porous breakwaters are introduced. The reflection and transmission coefficients between predictions and experimental results of authors' and four other researchers' are compared. By comparisons, the estimate methods of the linearized resistance coefficient f and the inertial effect coefficient s of the permeable plate are recommended. Following the formula of Yu [1995], the values of G are calculated by f and s. A complete estimate method of porous effect parameter G is presented, which consists of the formula of Yu [1995] and the present experimental formula. The estimate method of G is validated by comparing

*Corresponding author.

the predicted values of the total horizontal wave loads on the perforated caisson with the experimental results.

Keywords: Thin permeable wall; porous effect parameter; resistance coefficient; inertial coefficient.

1. Introduction

Recently, various vertical permeable breakwaters and docks have been gradually used in coastal engineering to reduce the wave load and the wave reflection in front of the structures. Compared with traditional coastal structures, the new forms are more economical for saving construction materials. They also bring smaller surface fluctuation in harbors due to the low reflection, which is much important for ship loading and unloading. And besides, the permeable breakwater allows water circulation, retains water quality and thus protects the coastal environment. In practices, there are two main forms of vertical permeable structures: (1) single or several vertical permeable plates [Yu, 1995; Isaacson *et al.*, 1998, 1999; McIver, 1999; Twu and Liu, 2004], (2) a solid back wall with single or several vertical permeable plates in front [Jarlan, 1961; Kondo, 1979; Tanimoto and Yoshimoto, 1982; Zhu and Chwang, 2001a]. Moreover, in the laboratories, a finite number of porous plates can be placed at the bottom of a wave tank to absorb waves [Twu and Lin, 1991; Losada *et al.*, 1993].

It is extremely complicated for wave motion through a permeable plate accompanied with the wave energy dissipation and phase shift. Thus, some assumptions are needed in the theoretical study. The method of assuming the permeable plate to be a rigid homogeneous porous medium is generally employed. For wave motion across a porous medium, the force exerted by the porous medium in fluid is described to include a resistance force corresponding to the linearized resistance coefficient f and an inertial force corresponding to the inertial effect coefficient s [Sollit and Cross, 1972]. Based on the porous medium hypothesis, Yu [1995] derived a porous boundary condition, through which the whole wave domain around the porous plate can be solved with analytical method [Isaacson *et al.*, 1998, 1999; Li *et al.*, 2003a; Teng *et al.*, 2004] or boundary element method [Cheng *et al.*, 2004; Zhao and Teng, 2004]. In the porous boundary condition, there is an important parameter named the porous effect parameter G [Yu, 1995]. The G is a complex number. The value of G depends on the geometrical parameters of the permeable plate and wave factors. The geometrical parameters of a permeable plate mainly consist of geometrical porosity, plate thickness and porous shape. The geometrical porosity is defined as the ratio of the volume occupied by the porous part (generally uniform) to the whole. The porosity is usually about 20% in practices [Zhu and Chwang, 2001a], but it can reach about 60% or higher as the first porous plate of a wave absorber in the wave flume [Twu and Lin, 1991]. For engineering practice, the thickness of porous wall is about 30–50 cm, and the plate thickness must satisfy the requirement of structural strength. There are several porous shapes in general

as follows: slit [Isaacson *et al.*, 1998, 1999; Tanimoto and Yoshimoto, 1982; Zhu and Chwang, 2001a], screen [Twu and Lin, 1991; Bennett *et al.*, 1992], circular holes [Kondo, 1979] and rectangular holes [Li *et al.*, 2002, 2003a, 2003b]. The value of G for a plate with certain geometrical parameters can be calculated by the resistance coefficient f and the inertial effect coefficient s, and the values of f and s must be obtained through experiments.

Another method based on a jet theory is also often used in studying wave interaction with permeable plates. When fluid passes an orifice in the permeable plate, the jet is formed. Then, the expanding and collision of jets from adjacent orifices can form two eddy zones behind the orifice. If the fluid oscillates, a rather thin eddy-effect region, as to compare with the incident wavelength, is formed around the plate. In the eddy-effect region, a head loss coefficient and an effective orifice length are used for expressing the resistance and inertial effect, respectively. Then another boundary condition on the permeable plate is developed. Mei *et al.* [1974] detailed this method. In the present study, porous medium hypothesis is followed.

It can be seen that lots of effective studies on the permeable wall structures have been carried out by different researchers. However, the precondition of these theoretical studies is to assume that the porous effect parameter G is known. Sometimes, it is also assumed that the resistance coefficient f and the inertial effect coefficient s are known, and then the G is calculated by them. Thus, in order to apply the numerical results to practices, explicit values of G or f and s must be obtained through experiments ahead. Now, comprehensive estimates of G or f and s are relatively scarce. Li *et al.* [2002, 2003b] have obtained the values of G with several given wave factors and geometrical parameters of the plates in their experiment. But the values can only be used on quite limited experimental conditions. In addition, some researchers [Losada *et al.*, 1993; Yu, 1995; Isaacson *et al.*, 1998, 1999; Zhu and Chwang, 2001b] have offered some values of f and s in their comparisons between numerical results and experimental data. However, these values are also just corresponding to a few limited experimental conditions. Therefore, the main intention of this paper is to find an effective and complete method to estimate the values of G through plenty of experimental data, which can be applied to engineering designs.

In the following section, the analytical solutions of wave interaction with two different vertical porous breakwaters are introduced. In Sec. 3, authors collect several other researchers' [Kondo, 1979; Tanimoto and Yoshimoto, 1982; Twu and Lin, 1991; Zhu and Chwang, 2001a] experimental data with the reflection coefficients of the permeable structures. Moreover, two different physical model experiments are also conducted. The reflection coefficient on a partially perforated caisson and the reflection and transmission coefficients of a porous plate are obtained under regular wave conditions. Then the values of f and s of porous plates with different geometrical parameters are obtained through comparing the predicted values of reflection coefficients with different experimental data. In this section, the total horizontal wave loads on the partially perforated caisson are also measured in the

present experiment. It will be used to validate the estimate method of G. In Sec. 4, the main effect factors of f are analyzed, and the formula for the calculation of f is recommended. The value of $s = 1$ is also recommended for the porous plate. Then the complete estimate method of G is obtained. The method consists of the present experimental formula and the formula of Yu [1995] for calculating G with f and s. The estimate method of G is validated by comparing the predicted values of the total horizontal wave loads on the partially perforated caisson with the experimental results. At last, the main conclusions of this paper are given.

2. Theoretical Methods

Let us consider the waves interacting with vertical permeable breakwaters. The idealized geometries of two typical breakwaters analyzed herein are shown as Fig. 1: (a) a single permeable plate extending from the seabed to above the water surface, (b) a caisson breakwater with a partially perforated front wall, a solid back wall and a wave chamber between them. A normally incident, regular, small amplitude wave train of wave height H, wave length L, angular frequency ω and wave period T approaches the structure. In Fig. 1(a), the water depth is constant d. In Fig. 1(b), the water depths outside and inside caisson are d and d_1, respectively, and the width of the wave chamber is B. The permeable plate thickness is b. The permeable plate thickness is considered in course of the derivation of porous boundary condition. However, the plate thickness is neglected in solving the fluid regions around the breakwater because it is very small compared with the wavelength and water depth.

2.1. *Single permeable plate*

As shown in Fig. 1(a), a Cartesian coordinate system (x, z) is defined with the origin at the intersection of the permeable plate and the still water level, the z-axis in the vertical direction upwards and the x-axis in the direction of wave propagation. The

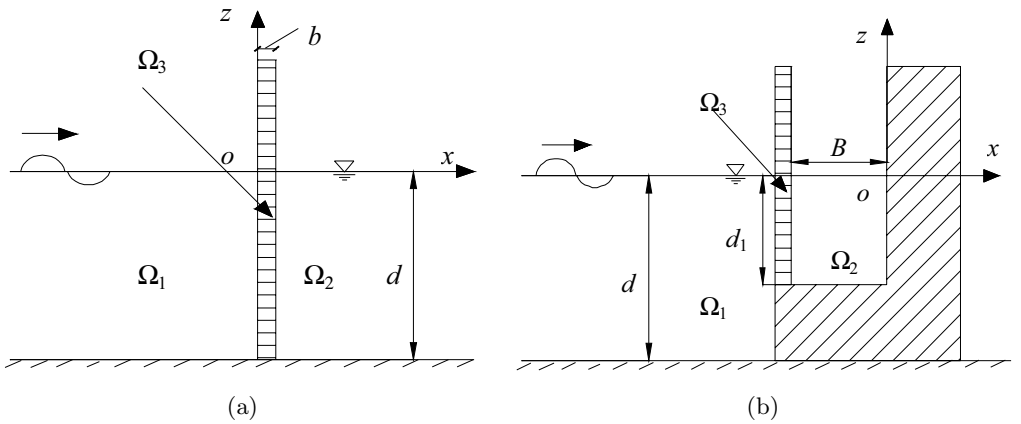

Fig. 1. Definition sketch: (a) Single permeable plate, (b) Partially perforated caisson breakwater.

whole fluid domain is divided into three regions for the convenience of solutions. The regions at the left-hand side, right-hand side and inside of the plate are called as Ω_1, Ω_2 and Ω_3. In the regions Ω_1 and Ω_2, the fluid is assumed to be inviscid and incompressible with the result that its motion is irrotational. For a monochromatic incident wave with an angular frequency ω, the time factor $e^{-\mathrm{i}\omega t}$ of the velocity potential can be extracted, and the velocity potential can be written as $\Phi(x, z, t) = \mathrm{Re}[\phi(x, z)e^{-\mathrm{i}\omega t}]$, where the $\phi(x, z)$ is a complex spatial potential. In order to solve $\phi(x, z)$ in the regions of Ω_1 and Ω_2, we can assumed the plate (region Ω_3) as a rigid homogeneous porous medium. Then, a porous boundary condition is derived by Yu [1995] as follows:

$$\frac{\partial \phi_1}{\partial x} = \frac{\partial \phi_2}{\partial x} = \mathrm{i}k_0 G(\phi_1 - \phi_2) \tag{1}$$

where ϕ_1 and ϕ_2 denote the spatial potentials in the regions Ω_1 and Ω_2; k_0 is the incident wave number, and satisfies the dispersion relation: $\omega^2 = gk_0 \tanh k_0 d$, in which g is the gravitational acceleration; G is the porous effect parameter and its values will be obtained in the present study. The process of the derivation is briefly introduced in Appendix A, and details can be found in Yu [1995]. By using this porous boundary condition, the reflection and transmission coefficients (K_r and K_t) of a single thin permeable plate are developed as follows [Yu 1995]:

$$K_r = \left| \frac{1}{1 + 2G} \right| \tag{2}$$

$$K_t = \left| \frac{2G}{1 + 2G} \right| \tag{3}$$

2.2. *Partially perforated caisson breakwater*

As shown in Fig. 1(b), a Cartesian coordinate system (x, z) is defined with the origin at the intersection of the wave chamber rear wall surface and the still water level, the z-axis in the vertical direction upwards and the x-axis in the direction out of the fluid domain. The whole fluid domain is divided into three regions. The Ω_1 and Ω_2 represent the regions outside and inside caisson, respectively. The region in the front perforated plate is called as Ω_3. Neglecting the thickness of region Ω_3, the fluid in regions Ω_1 and Ω_2 is assumed to be inviscid and incompressible with the result that its motion is irrotational. The spatial potentials in Ω_1 and Ω_2 satisfy Laplace equation:

$$\nabla^2 \phi_j = 0 \quad j = 1, 2 \tag{4}$$

where subscript j denotes the variables in region Ω_j.

Boundary conditions are given as follows.

Linearized free surface condition:

$$\frac{\partial \phi_j}{\partial z} = \frac{\omega^2}{g}\phi_j \quad j = 1, 2\,, \quad z = 0 \tag{5}$$

non-penetrating seabed conditions and impermeable solid back wall condition:

$$\frac{\partial \phi_1}{\partial z} = 0 \quad z = -d\,, \quad x \le -B \tag{6}$$

$$\frac{\partial \phi_2}{\partial z} = 0 \quad z = -d_1\,, \quad -B \le x \le 0 \tag{7}$$

$$\frac{\partial \phi_2}{\partial x} = 0 \quad -d_1 \le z \le 0\,, \quad x = 0 \tag{8}$$

radiation condition at $x \to -\infty$ for the reflected waves:

$$\frac{\partial \phi_r}{\partial x} = -\mathrm{i}k_0\phi_r \quad x \to -\infty \tag{9}$$

where ϕ_r is the reflection potential.

In regions Ω_1 and Ω_2, the spatial potentials that satisfy the above control equation and the boundary conditions can be developed by the separation of variables as follows:

$$\phi_1 = -\frac{\mathrm{i}gH}{2\omega}\left[Z_0 e^{\mathrm{i}k_0(x+B)} + Z_0 R_0 e^{-\mathrm{i}k_0(x+B)} + \sum_{m=1}^{\infty} R_m Z_m e^{k_m(x+B)}\right] \quad m = 1, 2, \ldots \tag{10}$$

$$\phi_2 = -\frac{\mathrm{i}gH}{2\omega}\left[Y_0 A_0 \cos\lambda_0 x + \sum_{n=1}^{\infty} Y_n A_n \frac{\cosh\lambda_n x}{\cosh\lambda_n B}\right] \quad n = 1, 2, \ldots \tag{11}$$

where the first part in the right-hand of Eq. (10) represents the incident waves propagating in the positive x-direction, the second part represents the reflected waves propagating in the negative x-direction in region Ω_1, and the third part represents a series of evanescent modes that decay in the negative x-direction in region Ω_1. The wave numbers k_0 and k_m, λ_0 and λ_n satisfy dispersion relations $\omega^2 = gk_0 \tanh k_0 d = -gk_m \tan k_m d$ and $\omega^2 = g\lambda_0 \tanh \lambda_0 d_1 = -g\lambda_n \tan \lambda_n d_1$, respectively. Z_0, Z_m, Y_0 and Y_n are eigenfunctions in the z-direction as follows:

$$Z_0 = \frac{\cosh k_0(z+d)}{\cosh k_0 d}\,, \quad Z_m = \frac{\cos k_m(z+d)}{\cos k_m d} \tag{12}$$

$$Y_0 = \frac{\cosh \lambda_0(z+d_1)}{\cosh \lambda_0 d_1}\,, \quad Y_n = \frac{\cos \lambda_n(z+d_1)}{\cos \lambda_n d_1} \tag{13}$$

They are complete orthogonal sets, with

$$\int_{-d}^{0} Z_i Z_j dz = \begin{cases} \dfrac{1}{\cosh^2 k_0 d}\left(\dfrac{d}{2}+\dfrac{\sinh 2k_0 d}{4k_0}\right) & i=j=0 \\ \dfrac{1}{\cos^2 k_m d}\left(\dfrac{d}{2}+\dfrac{\sin 2k_m d}{4k_m}\right) & i=j=m=1,2\ldots \\ 0 & i\neq j \end{cases}$$

$$\int_{-d_1}^{0} Y_i Y_j dz = \begin{cases} \dfrac{1}{\cosh^2 \lambda_0 d_1}\left(\dfrac{d_1}{2}+\dfrac{\sinh 2\lambda_0 d_1}{4\lambda_0}\right) & i=j=0 \\ \dfrac{1}{\cos^2 \lambda_n d_1}\left(\dfrac{d_1}{2}+\dfrac{\sin 2\lambda_n d_1}{4\lambda_n}\right) & i=j=n=1,2\ldots \\ 0 & i\neq j \end{cases} \tag{14}$$

R_0, R_m, A_0 and A_n are the unknown expansion coefficients, and they can be determined by matching the following porous boundary conditions at the perforated front wall:

$$\frac{\partial \phi_1}{\partial x} = \frac{\partial \phi_2}{\partial x} = \mathrm{i}k_0 G(\phi_1 - \phi_2) \quad -d_1 \le z \le 0\,, \quad x = -B \tag{15}$$

$$\frac{\partial \phi_1}{\partial x} = 0 \quad -d \le z \le -d_1\,, \quad x = -B \tag{16}$$

The matching method has been explained in detail in another paper [Li *et al.*, 2002], and is omitted here. For the linear wave theory, the reflection coefficient for a partially perforated caisson breakwater can be obtained as

$$K_r = |R_0| \tag{17}$$

The wave pressure p can be calculated according to the linearized Bernoulli Equation $p(x,z) = \mathrm{i}\omega\rho\phi(x,z)$. Then the horizontal wave load can be obtained by integrating the wave pressures on the caisson. The total horizontal wave load consists of three parts that are wave load F_1 due to the pressure difference on the perforated front plate, F_2 on the solid part of the breakwater front surface and F_3 on the solid back wall. They are written as follows:

$$F_1 = \frac{\rho g H}{2\mathrm{i}k_0 G}\left(A_0 \sin\lambda_0 B \frac{\sinh\lambda_0 d_1}{\cosh\lambda_0 d_1} - \sum_{n=1}^{\infty} \frac{\sinh\lambda_n B}{\cosh\lambda_n B}\cdot\frac{\sin\lambda_n d_1}{\cos\lambda_n d_1}\right) \tag{18}$$

$$F_2 = \frac{\rho g H}{2}\left[(1+R_0)\frac{\sinh k_0(d-d_1)}{k_0\cosh k_0 d} + \sum_{m=1}^{\infty} R_m \frac{\sin k_m(d-d_1)}{k_m \cos k_m d}\right] \tag{19}$$

$$F_3 = \frac{\rho g H}{2}\left(A_0 \frac{\sinh\lambda_0 d_1}{\lambda_0\cosh\lambda_0 d_1} + \sum_{n=1}^{\infty} A_n \frac{\sin\lambda_n d_1}{\lambda_n \cos\lambda_n d_1}\cdot\frac{1}{\cosh\lambda_n B}\right) \tag{20}$$

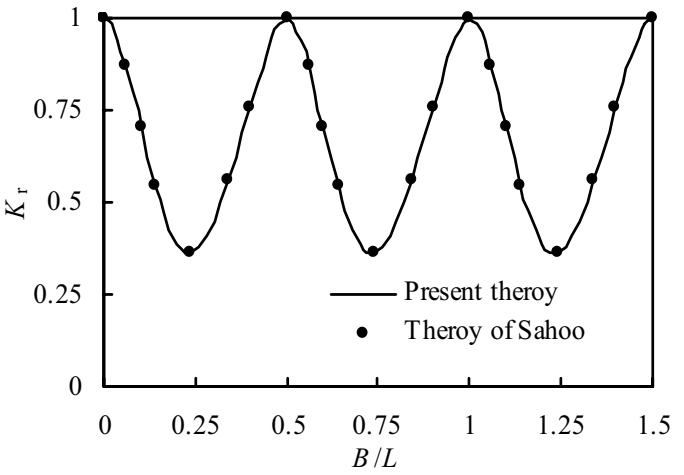

Fig. 2. Comparison between Sahoo *et al.* [2000] and present theory, $k_0 = 2.0$, $G = 2.0 + 0.5\mathrm{i}$.

By considering a fully perforated caisson i.e. the water depth inside caisson is equal to that outside, the reflection coefficient of normally incident wave is given by Sahoo *et al.* [2000] as follows:

$$K_r = \frac{1 - G(1 - \mathrm{i}\cot k_0 B)}{1 + G(1 + \mathrm{i}\cot k_0 B)} \tag{21}$$

The results of reflection coefficient of fully perforated caisson calculated with Eqs. (17) and (21), respectively, are exactly the same as shown in Fig. 2, as a function of relative wave chamber width i.e. the ratio of the wave chamber width to the incident wavelength B/L for $k_0 = 2.0$, $G = 2.0 + 0.5\mathrm{i}$.

3. Values of Parameters f and s

According to Appendix A, the values of porous effect parameter G can be calculated by the following formula:

$$G = G_r + \mathrm{i}G_i = \frac{\varepsilon}{k_0 b(f - \mathrm{i}s)} \tag{22}$$

where the porosity ε, the plate thickness b and the incident wave number k_0 are known. We can get the values of G if the values of the resistance coefficient f and the inertial effect coefficient s are obtained. The inertial coefficient s can be related to an added mass coefficient C_m by

$$s = 1 + C_m \left(\frac{1 - \varepsilon}{\varepsilon}\right) \tag{23}$$

For porous structures consisting of gravels, the value of $C_m = 0.34$ has been recommended by van Gent [1995] and Requejo *et al.* [2002] based on oscillatory flow experiments. However, many researchers [e.g. Sollit and Cross, 1972; Losada *et al.*, 1993;

Yu, 1995; Isaacson *et al.*, 1998, 1999; Zhu and Chwang, 2001b; Hossain *et al.*, 2001] have used the value of $C_m = 0$ i.e. $s = 1$ for comparing the numerical predictions of reflection and transmission coefficients of permeable structures with experimental results. The comparisons are also quite well. If C_m is zero, the imaginary part of G should be generally small. In fact, the most values of G's imaginary part obtained by Li *et al.* [2002, 2003b] are much smaller, and can be neglected. When the inertial effect is neglected, the G is reduced to be a real number defined by Chwang [1983]. It is just based on the past studies mentioned above that, initially, the values of $C_m = 0$ and 0.34 are both considered in this paper. However, it is found from our initial calculations that the value of $C_m = 0$ ($s = 1$) is more suitable for predicting the reflection and transmission coefficients of permeable wall structures. Thus, in the following text, only some typical predicted results with $C_m = 0.34$ are given as the comparisons with the predicted results with $C_m = 0$. For calculating G, the values of f also need to be determined. In the original formulation of Sollit and Cross [1972], the values of f are calculated implicitly using the Lorentz principle of equivalent work, and an iterative procedure is required. But an iterative calculation is unfeasible when we use the porous boundary condition to solve velocity potentials in the regions around breakwaters. Thus, the values of f need to be given ahead. Previous researchers [Losada *et al.*, 1993; Isaacson *et al.*, 1998, 1999; Yu, 1995; Zhu and Chwang, 2001b] usually calculate the reflection coefficients of the permeable structures with different values of f firstly. Then the predicted values are compared with the experimental results, and the values of f are estimated on the basis of a best fit between the predicted values and experimental results. But the estimated values are just corresponding to a few limited experimental conditions. To the best of the authors' knowledge, a uniform criterion and systematic discussions of the values of f cannot be found in the published literatures, which bring lots of difficulties in practical application. In the following study, the values of f will be estimated systematically on the basis of the least square method between predicted values of the reflection coefficients and a lot of experimental data from different researchers. If there is no special explanation, the value of $s = 1$ is used in the following comparisons.

The predicted values of reflection coefficients are firstly compared with four previous experimental results [Kondo, 1979; Tanimoto and Yoshimoto, 1982; Twu and Lin, 1991; Zhu and Chwang, 2001a]. The model geometrical parameters and testing conditions of these experiments are all listed in Table 1.

Tanimoto and Yoshimoto [1982] conducted a physical model test to examine the reflection coefficients of caissons with different partially slit front walls. The experiment was carried out in a wave tank 39.5 m long, 1.27 m deep and 1 m wide in the domain of wave maker side, 0.97 m deep and 0.48 m wide in the domain of lee side. The present predictions are compared with the results of this experiment, and some optimum values of f are obtained. Figure 3 shows comparisons of the measured and predicted reflection coefficients as a function of B/L_1 (wave chamber

Table 1. Model geometrical parameters and testing conditions of previous experiments.

Experiments	Tanimoto [1982]	Twu [1991]	Kondo [1979]	Zhu [2001a]
Wave period T (s)	0.85–3.00	0.85–3.00	0.7–2.1	0.5–1.0
Wave height H (cm)	3.3–22.5	2–4	4	3
Water depth d (cm)	60	50	50	32
Water depth d_1 (cm)	20–60	50	50	32
Wave chamber width B (cm)	17–97	44	50	2.4–48.4
Porosity ε	0.143, 0.25, 0.333, 0.4	0.58	0.2, 0.34	0.2
Plate thickness b (cm)	3.0, 6.0, 9.0	2.4	0.6	0.3
Porous shape	slit	screen	circular holes	slit

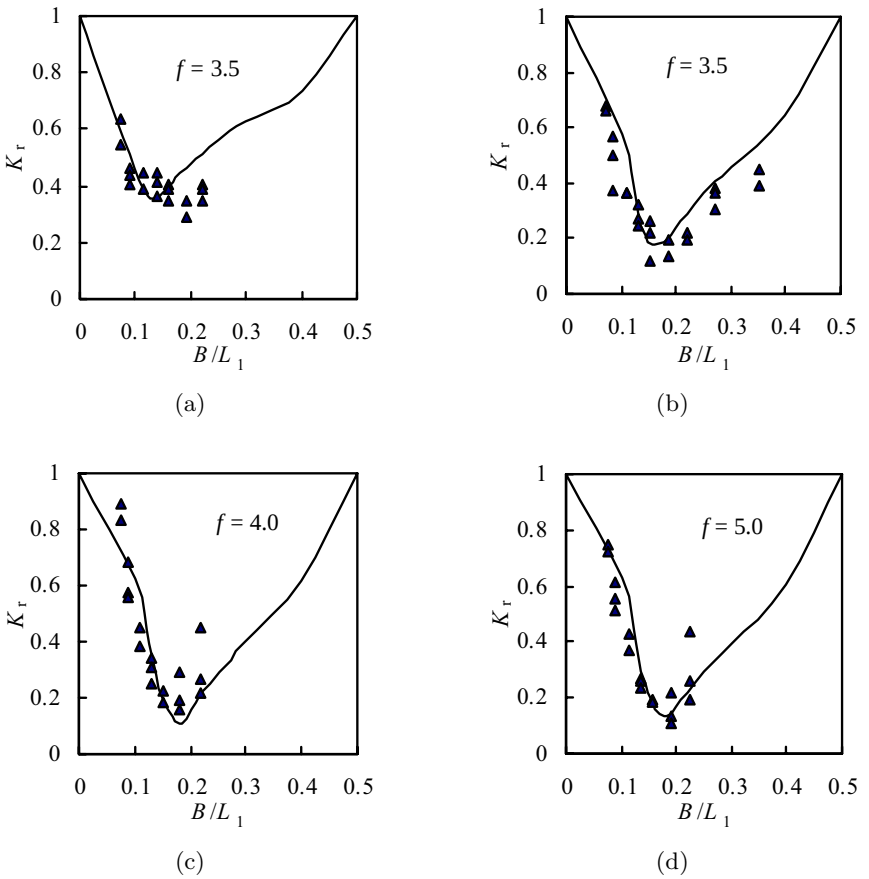

Fig. 3. Comparisons of predicted K_r with experimental results of Tanimoto and Yoshimoto [1982] as function of B/L_1: (a) $\varepsilon = 0.143$; (b) $\varepsilon = 0.25$; (c) $\varepsilon = 0.333$; (d) $\varepsilon = 0.4$; $b/d = 0.05$, $B/d = 0.617$, $d_1/d = 0.5$; ▲, measured; ——, predicted.

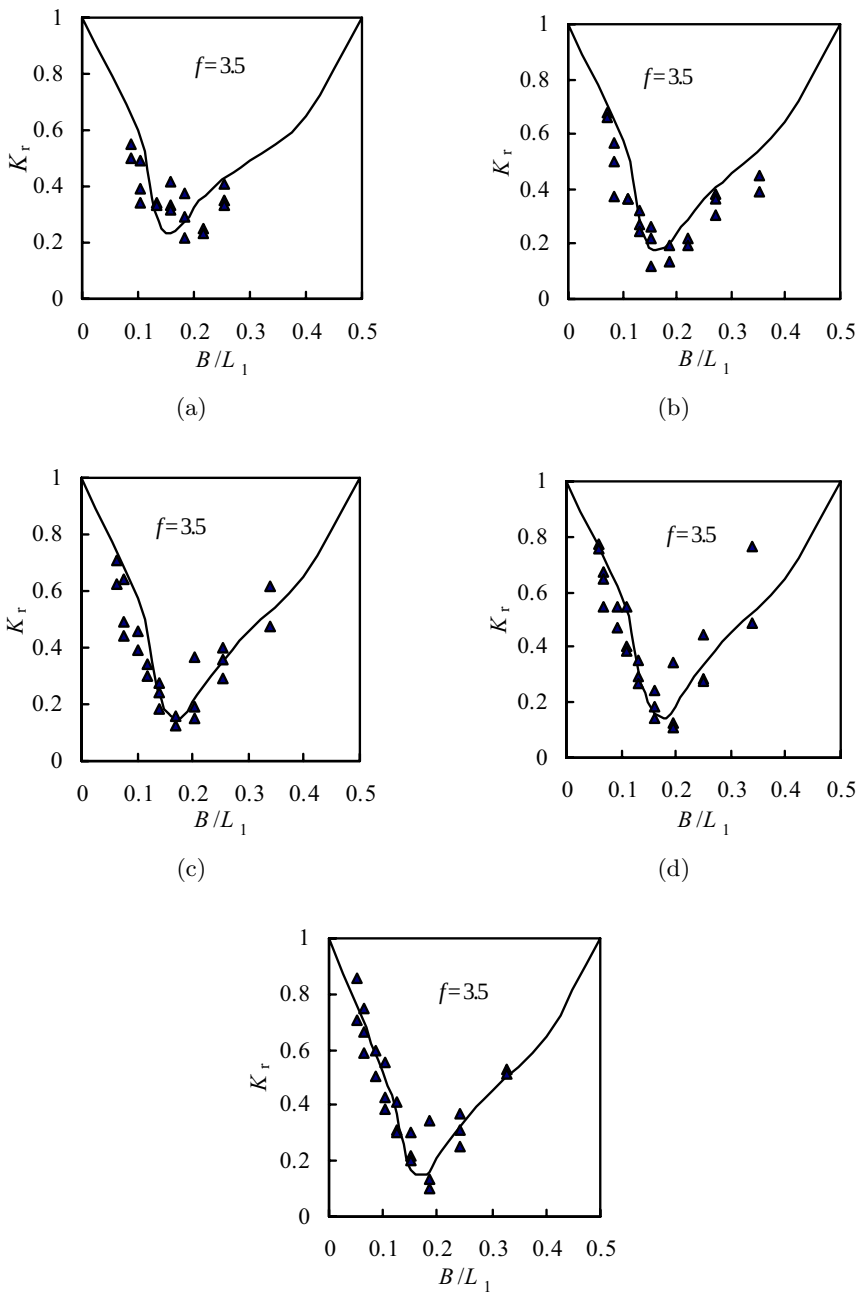

Fig. 4. Comparisons of predicted K_r with experimental results of Tanimoto and Yoshimoto [1982] as function of B/L_1: (a) $d_1/d = 0.333$; (b) $d_1/d = 0.5$; (c) $d_1/d = 0.667$; (d) $d_1/d = 0.833$; (e) $d_1/d = 1.0$; $b/d = 0.05$, $B/d = 0.617$, $\varepsilon = 0.25$; ▲, measured; ——, predicted.

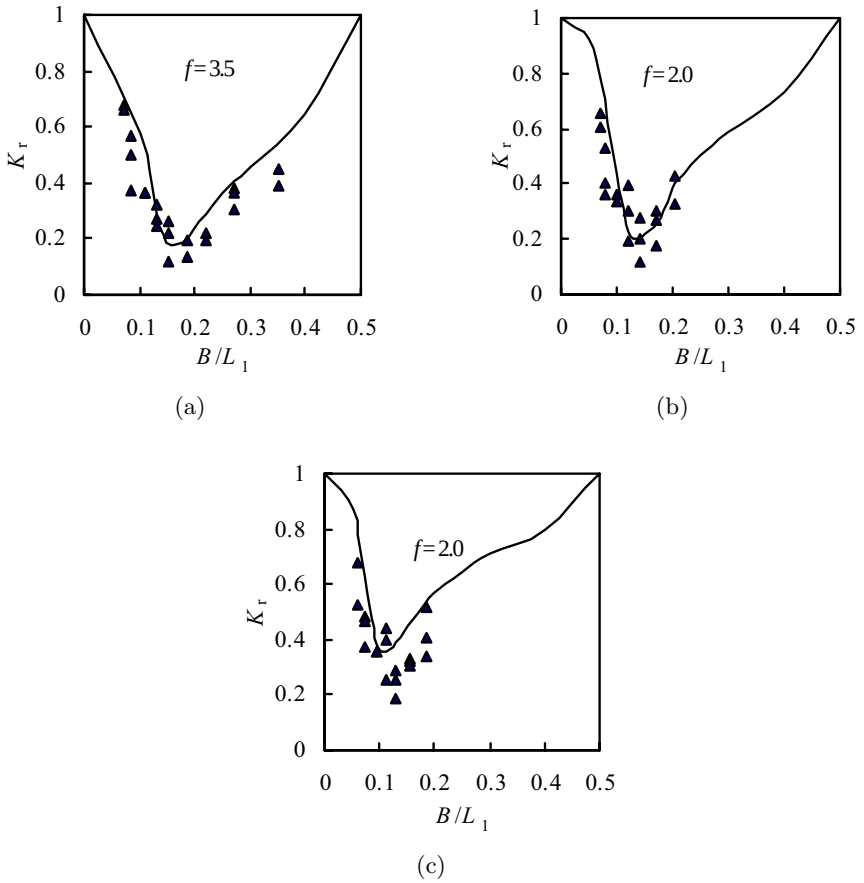

Fig. 5. Comparisons of predicted K_r with experimental results of Tanimoto and Yoshimoto [1982] as function of B/L_1: (a) $b/d = 0.05$, $B/d = 0.617$; (b) $b/d = 0.1$, $B/d = 0.567$; (c) $b/d = 0.15$, $B/d = 0.517$; $\varepsilon = 0.25$, $d_1/d = 0.5$; ▲, measured; ——, predicted.

width/wavelength in wave chamber) for relative slit front wall thickness $b/d = 0.05$, $B/d = 0.617$, $d_1/d = 0.5$ and porosities $\varepsilon = 0.143$, 0.25, 0.333 and 0.4. The best optimum values of f are 3.5 for $\varepsilon = 0.143$ and 0.25, 4.0 for $\varepsilon = 0.333$ and 5.0 for $\varepsilon = 0.4$. The estimated f are all 3.5 with $b/d = 0.05$, $B/d = 0.617$, $\varepsilon = 0.25$ and $d_1/d = 0.333$, 0.5, 0.667, 0.833 and 1.0, as shown in Fig. 4. The values of f are 3.5, 2 and 2 with $\varepsilon = 0.25$, $d_1/d = 0.5$, b/d and $B/d = 0.05$ and 0.617, 0.1 and 0.567 and 0.15 and 0.517, as shown in Fig. 5. It can be seen that the values of f are smaller ($f = 2.0$) for larger relative slit wall thickness ($b/d = 0.1$ and 0.15). The same $f(f = 2.0)$ also has been obtained by Yu [1995] for the rubble structures.

Twu and Lin [1991] also conducted a test to get the reflection coefficient of a wave absorber consisting of a solid back wall, a front screen and a wave chamber between them. The experiment was conducted in a 75 m long wave flume with a cross section of 1.2×1.0 m. The relative thickness b/d of the front wave screen is 0.048, and the porosity is 0.58. The predicted reflection coefficients and the experimental results

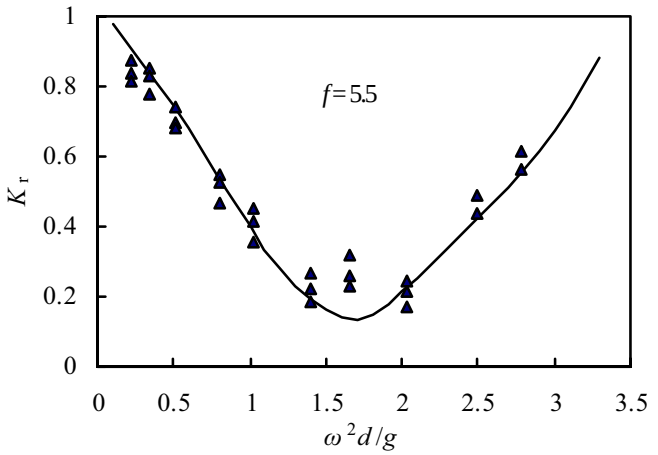

Fig. 6. Comparison of predicted K_r with experimental results of Twu and Lin [1991] as function of $\omega^2 d/g$: $b/d = 0.048$, $\varepsilon = 0.58$; ▲, measured; ——, predicted.

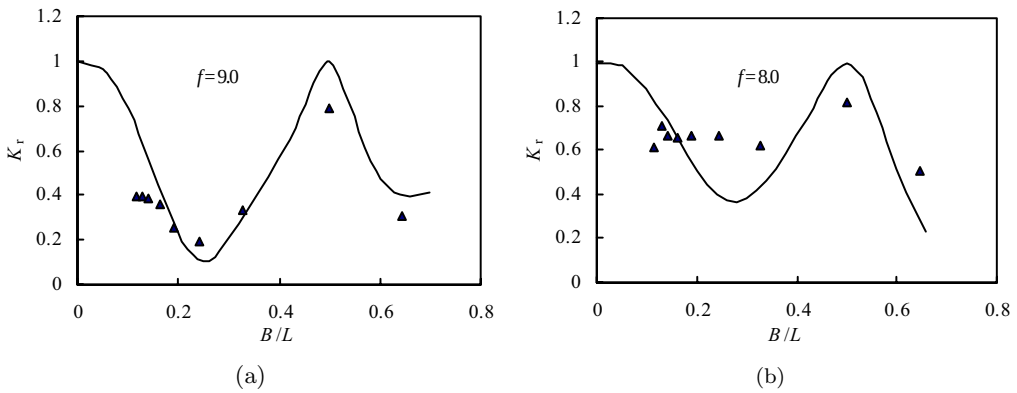

Fig. 7. Comparisons of predicted reflection coefficient K_r with experimental results of Kondo [1979] as function of B/L: (a) $\varepsilon = 0.2$; (b) $\varepsilon = 0.34$; $b/d = 0.012$; ▲, measured; ——, predicted.

as a function of relative water depth $\omega^2 d/g$ are reproduced most well when f is 5.5, as shown in Fig. 6. In fact, the basic conditions of this experiment are very similar to Tanimoto and Yoshimoto's [1982], and the estimated value of f is also close to that of Tanimoto and Yoshimoto [1982] with a porosity $\varepsilon = 0.4$ [Fig. 3(d), $f = 5.0$]. Losada *et al.* [1993] and Zhu and Chwang [2001b] also compared their numerical results with this experiment, and obtained the same f of 5.5 with the present study.

Kondo [1979] measured the reflection coefficient of a perforated breakwater with single chamber under regular wave attack in a wave flume of 18.5 m long, 0.4 m wide and 1.0 m deep. The relative perforated wall thickness b/d is 0.012, and the porosities are 0.2 and 0.34, respectively. The estimated results of f are shown in Fig. 7, where the best agreements are obtained when f is 9.0 with the porosity of 0.2, and 8.0 with the porosity of 0.34.

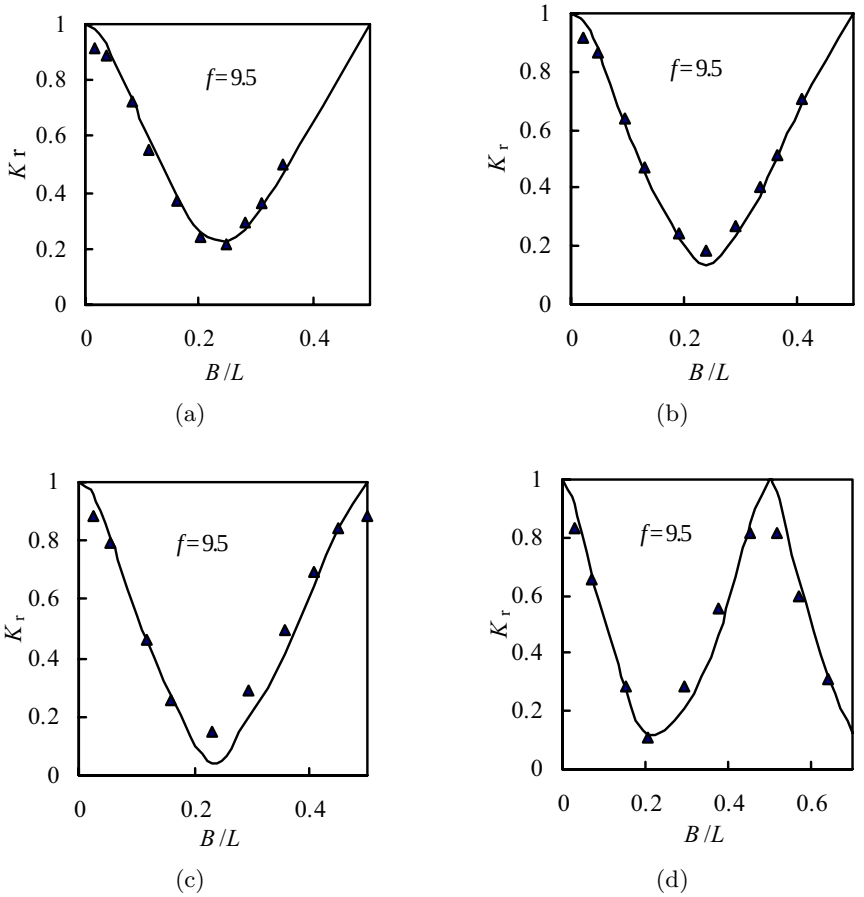

Fig. 8. Comparisons of predicted reflection coefficient K_r with experimental results of Zhu and Chwang [2001a] as function of B/L: (a) $k_0 d = 1.44$; (b) $k_0 d = 1.70$; (c) $k_0 d = 2.08$; (d) $k_0 d = 2.66$; $b/d = 0.0094$, $\varepsilon = 0.2$; ▲, measured; ——, predicted.

Zhu and Chwang [2001a] conducted a physical model test to investigate the reflection coefficient of a slotted seawall consisting of a slotted plate, a solid back wall and a wave chamber between them. The experiment was conducted in a wave flume of 12 m long, 0.3 m wide and 0.45 m deep with glass walls. The relative slotted plate thickness b/d is 0.0094, and the porosity is 0.2. The best fit f value is 9.5 for this experiment, as shown in Fig. 8.

Authors also conducted a physical model test to measure reflection coefficients and total horizontal wave loads on partially perforated caissons. The experiment was carried out in a wave-current flume in the State Key Laboratory of Coastal and Offshore Engineering, Dalian University of Technology, China. The wave flume is 56 m long, 0.7 m wide and 1.0 m deep, equipped with a computer-controlled irregular wave maker. The wave maker can generate waves with periods of 0.5–5 s. The models are made of plexiglass, and consist of three caissons. One of them is used for measuring the horizontal wave load with 0.45 m long, 0.22 m wide and 0.75 m

Table 2. Model geometrical parameters and testing conditions of present perforated caisson experiment.

Wave period T (s)	0.86	1.0		1.2	1.4
Wave height H (cm)	6, 8	6, 8, 10, 12		6, 8, 10, 12	6, 8, 10, 12
Chamber width B (cm)	15		20		30
Caisson porosity ε	0.2			0.4	
Water depth d (cm)			40		
Water depth d_1 (cm)			20		
Plate thickness (cm)			1.0		
Porous shape			rectangular holes		

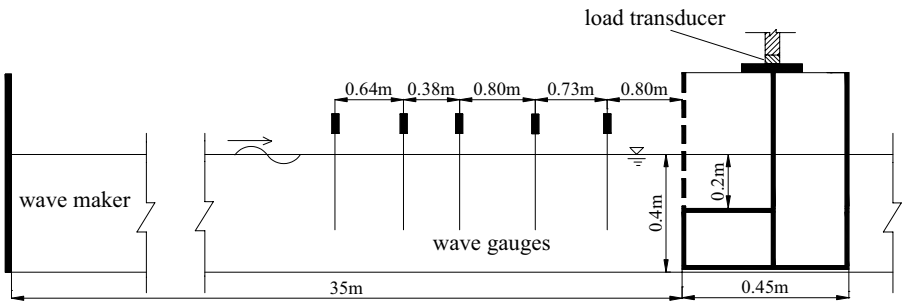

Fig. 9. Experimental set-up of perforated caissons.

high, and the rest two are assistant models with 0.45 m long, 0.226 m wide and 0.75 m high. The front plates are partially perforated with uniform rectangular holes. The perforated position begins from 0.2 m leaving the model bottom upward to the top of the wall. The relative perforated plate thickness b/d is 0.025, and the porosities are 0.2 and 0.4. The model geometrical parameters and testing conditions are listed in Table 2. The experimental set-up is shown in Fig. 9. The middle caisson ($45 \times 22 \times 75$ cm) is hung up through a load transducer fixed on the steel structure located on the top of the wave flume. The distances between the middle caisson and assistant models on both sides are about 0.5 cm. The middle caisson must avoid contacting around during the test for the accuracy of wave load measurement. Five wave gauges arranged along the axis of the wave flume are used for measuring the free surface elevations in front of the models. A computer control system is used for collecting the data of free surface elevations and wave loads. The test should be terminated before the re-reflected waves reach the models. There are no overtopping and wave breaking in the experiment. Goda's Method [Goda and Suzuki, 1976] is used for estimating the reflection coefficient. For this method, the distance between two wave gauges should not be an integer multiple of the half-wavelength, and a reasonable distance is 0.05–0.45 multiple wavelength. The reflection coefficients are estimated by using suitable pairs of wave gauges for different wavelengths. The

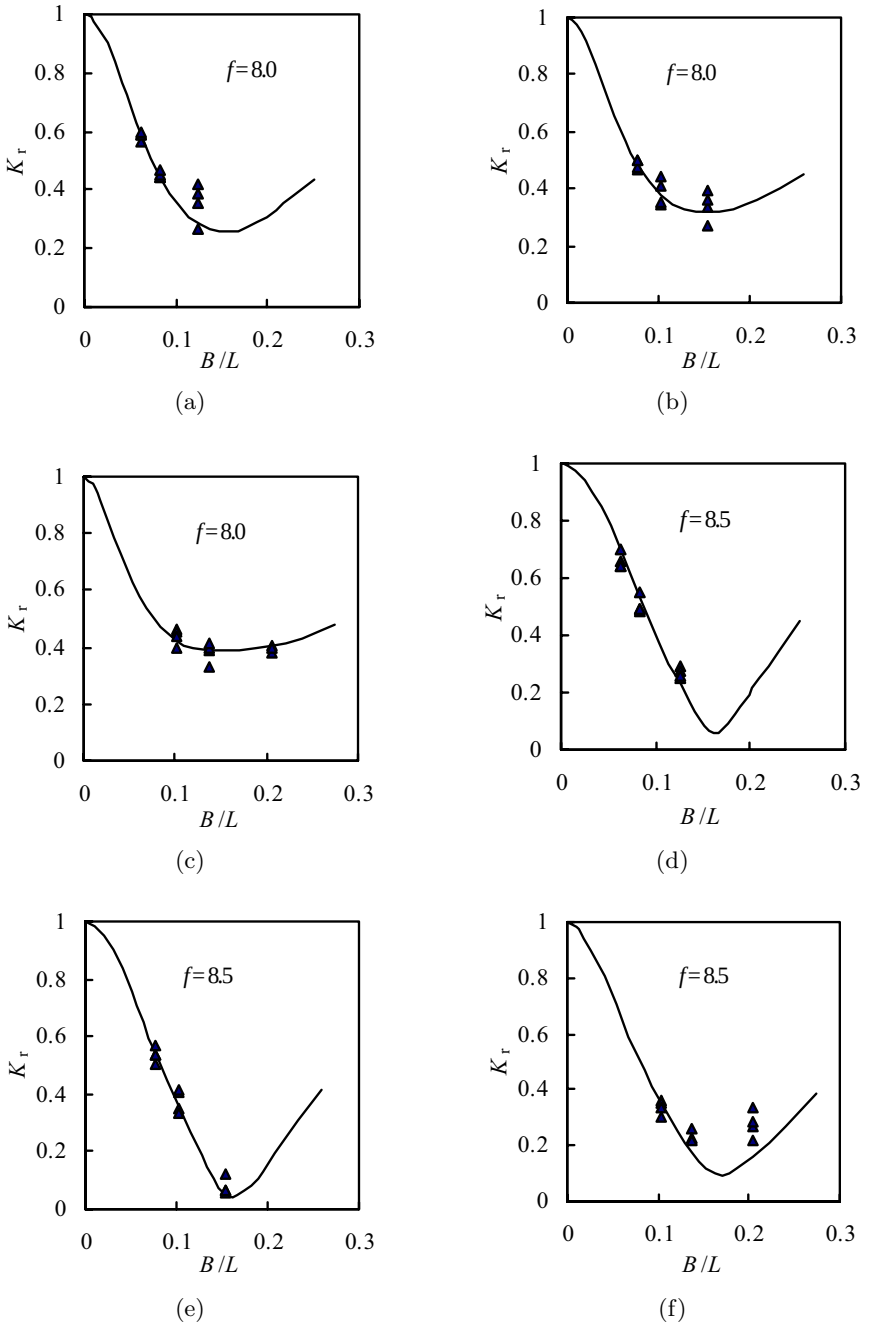

Fig. 10. Comparisons of predicted K_r with experimental results of perforated caissons as function of B/L: (a) $\varepsilon = 0.2$, $k_0 d = 1.05$; (b) $\varepsilon = 0.2$, $k_0 d = 1.30$; (c) $\varepsilon = 0.2$, $k_0 d = 1.72$; (d) $\varepsilon = 0.4$, $k_0 d = 1.05$; (e) $\varepsilon = 0.4$, $k_0 d = 1.30$; (f) $\varepsilon = 0.4$, $k_0 d = 1.72$; $b/d = 0.025$; ▲, measured; ——, predicted.

comparisons between predicted and experimental results of reflection coefficient K_r as a function of relative wave chamber width B/L are shown in Fig. 10, where the best fit f values are 8.0 for a porosity of 0.2 and 8.5 for a porosity of 0.4.

The porous shapes of the plates are different (including slit, screen, circular holes and rectangular holes) in all the above experiments. In order to analyze the effects of porous shape and porosity on the values of f, authors conducted another experiment to measure the reflection and transmission coefficients of a thin vertical porous plate with different porous shapes and porosities. The experiment was performed in another wave-current flume in the State Key Laboratory of Coastal and Offshore Engineering, Dalian University of Technology, China. The wave flume is 69 m long, 2 m wide and 1.8 m deep. It is equipped with an irregular wave maker made by the MTS company. The wave maker can generate waves with periods of 0.5–5 s. The wave flume is divided into two regions (0.8 m wide and 1.2 m wide) by a thin board from about 40 m leaving the wave maker to the bottom. The 0.8 m wide region was used in our experiment. The porous plate made of plexiglass is 1 cm thick,

Table 3. Model geometrical parameters and testing conditions of present porous plate experiment.

	$T = 0.95$ s	1.0 s	1.2 s	1.4 s	1.6 s	1.8 s	2.0 s
$H = 6$ cm					✓	✓	✓
8 cm	✓	✓	✓	✓	✓	✓	✓
10 cm		✓	✓	✓	✓	✓	✓
12 cm			✓	✓			
Porous shape		slit		string		circular holes	
Porosity ε		0.1, 0.2, 0.3, 0.4		0.2		0.2	
Water depth d (cm)				35			
Plate thickness b (cm)				1.0			

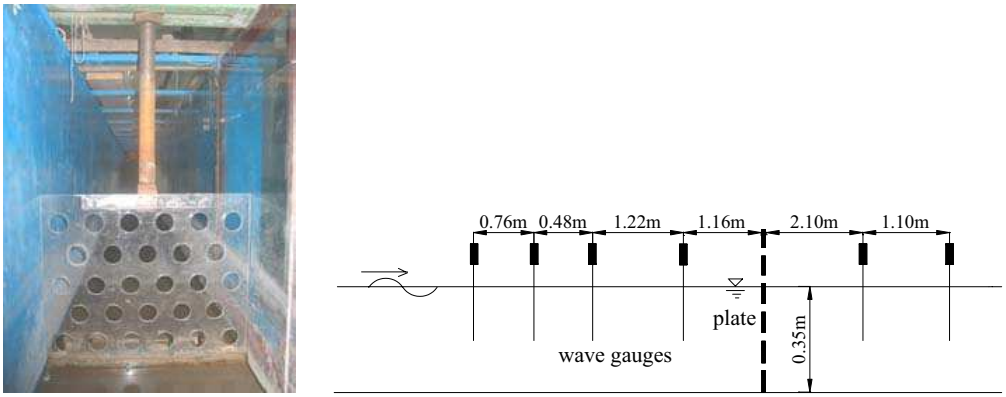

(a) (b)

Fig. 11. Experimental set-up of a porous plate: (a) photo of a plate in the wave flume; (b) arrangements of wave gauges.

0.8 m wide and 0.7 m high. There are three different porous shapes: slit ($\varepsilon = 0.1$, 0.2, 0.3 and 0.4), string ($\varepsilon = 0.2$) and circular holes ($\varepsilon = 0.2$). In this experiment, the relative plate thickness b/d is 0.0286. The experimental conditions are listed in Table 3. The experimental set-up is given in Fig. 11. The plate is located about 45 m far from the wave maker. Four wave gauges are arranged before the plate along the

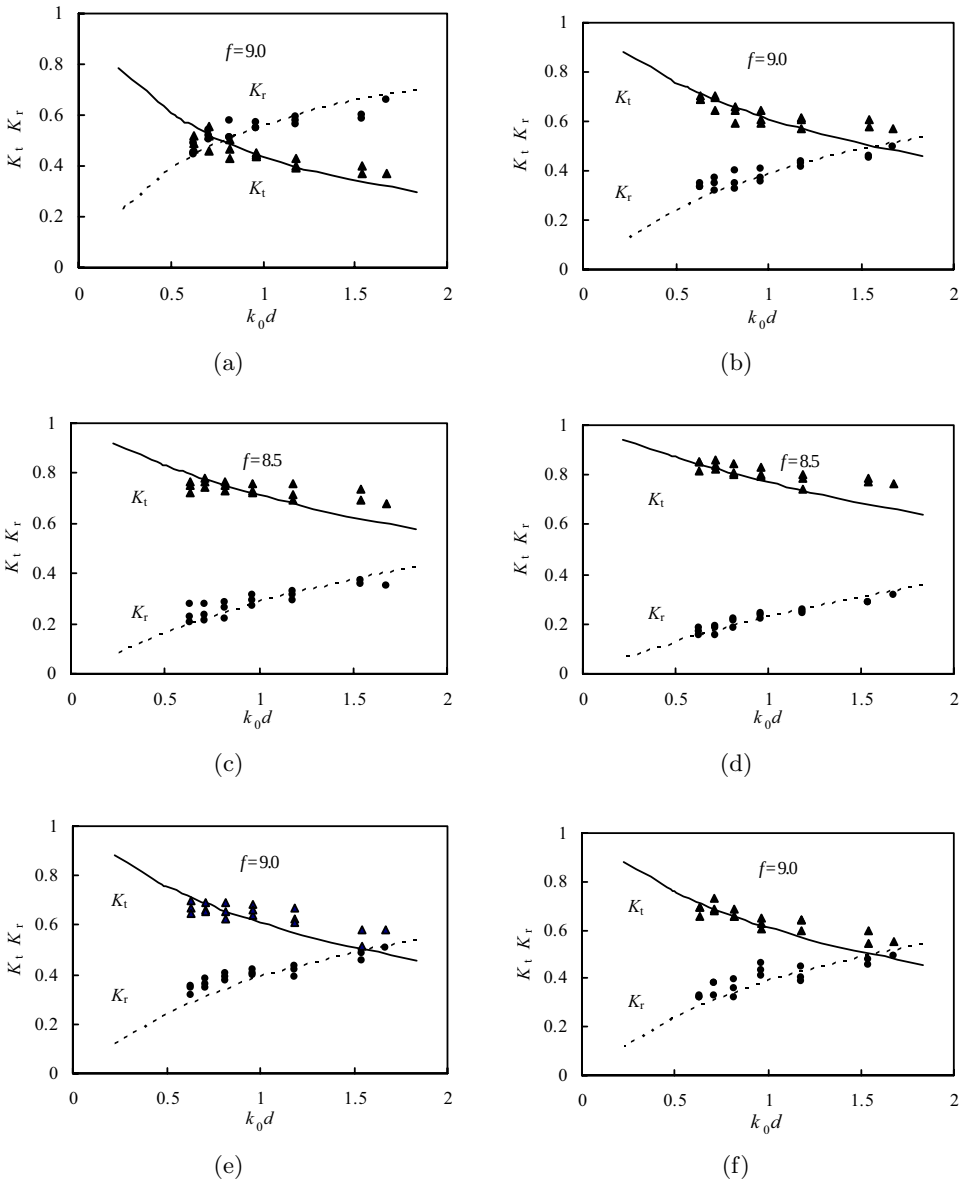

Fig. 12. Comparisons of predicted K_t and K_r with experimental results of the porous plate as function of k_0d: (a) $\varepsilon = 0.1$, slit; (b) $\varepsilon = 0.2$, slit; (c) $\varepsilon = 0.3$, slit; (d) $\varepsilon = 0.4$, slit; (e) $\varepsilon = 0.2$, string; (f) $\varepsilon = 0.2$, circular holes; $b/d = 0.0286$; K_t: ▲, measured; ——, predicted; K_r: •, measured; – – –, predicted.

axis of the wave flume to measure the free surface elevations. The transmitted wave heights are also measured by other two wave gauges arranged behind the plate. The data are collected by a computer control system. The test should be terminated before the rereflected waves reaching the plate. There are no overtopping and wave breaking in the experiment, and the transmitted waves are well absorbed by the wave absorbing system arranged at the end of the wave flume. The Goda's Method [Goda and Suzuki, 1976] is also used for estimating reflection and transmission coefficients with suitable pairs of wave gauges. Figure 12 shows comparisons of the measured and predicted transmission and reflection coefficients as a function of $k_0 d$ with the best optimum values of f. It is found that the best fit values of f are 9.0 with porosities of 0.1 and 0.2, and 8.5 with porosities of 0.3 and 0.4.

As mentioned at the beginning of this section, the value of $C_m = 0.34$ recommended by van Gent [1995] and Requejo *et al.* [2002] has also been used for predicting the reflection and transmission coefficients of permeable wall structures. Some best fit results between numerical and experimental data are given in Figs. 13–15. In

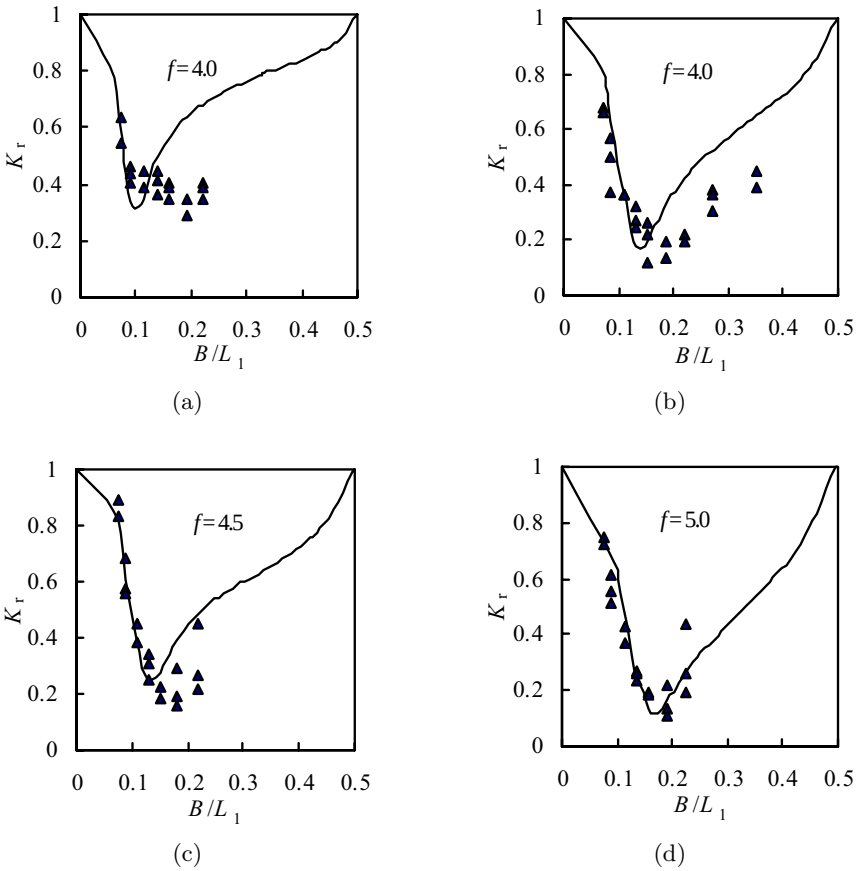

Fig. 13. Comparisons of predicted K_r with experimental results of Tanimoto and Yoshimoto [1982] as function of B/L_1 : $C_m = 0.34$; other conditions are same with Fig. 3.

general, for different C_m, the good agreements between predictions and experimental results can all be obtained with suitable values of f (comparing Fig. 14 with Fig. 6 and Fig. 15 with Fig. 10). However, for larger relative plate thickness ($b/d = 0.05$) with moderate porosities ($\varepsilon = 0.143,\ 0.25,\ 0.333$), the value of $C_m = 0$ is more suitable for predicting the reflection coefficients of perforated caissons (comparing Fig. 13 with Fig. 3). Thus, $C_m = 0$ ($s = 1$) is recommended for thin permeable plates.

4. Discussion and Analysis

The values of f with different conditions are obtained according to plenty of comparisons between predictions and experimental results. At the same time, the value

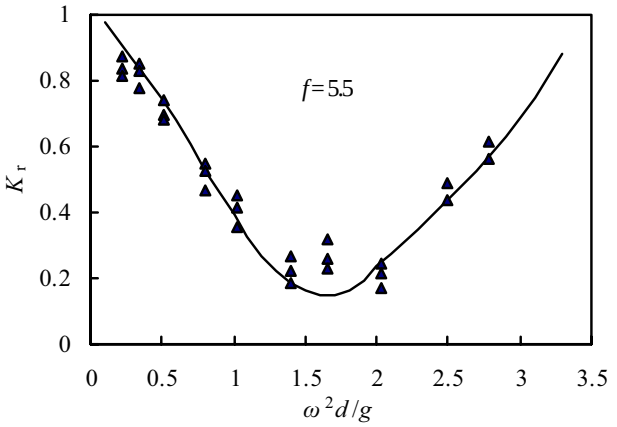

Fig. 14. Comparison of predicted K_r with experimental results of Twu and Lin [1991] as function of $\omega^2 d/g$: $C_m = 0.34$; other conditions are same with Fig. 6.

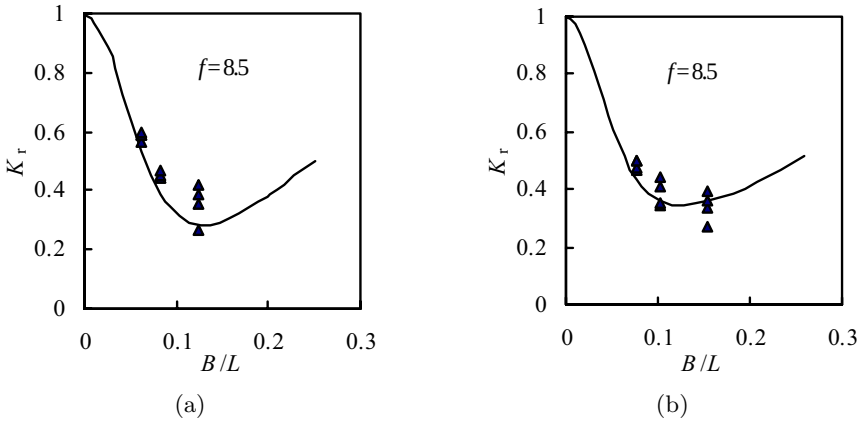

Fig. 15. Comparisons of predicted K_r with experimental results of perforated caissons as function of B/L : $C_m = 0.34$; other conditions are same with Fig. 10.

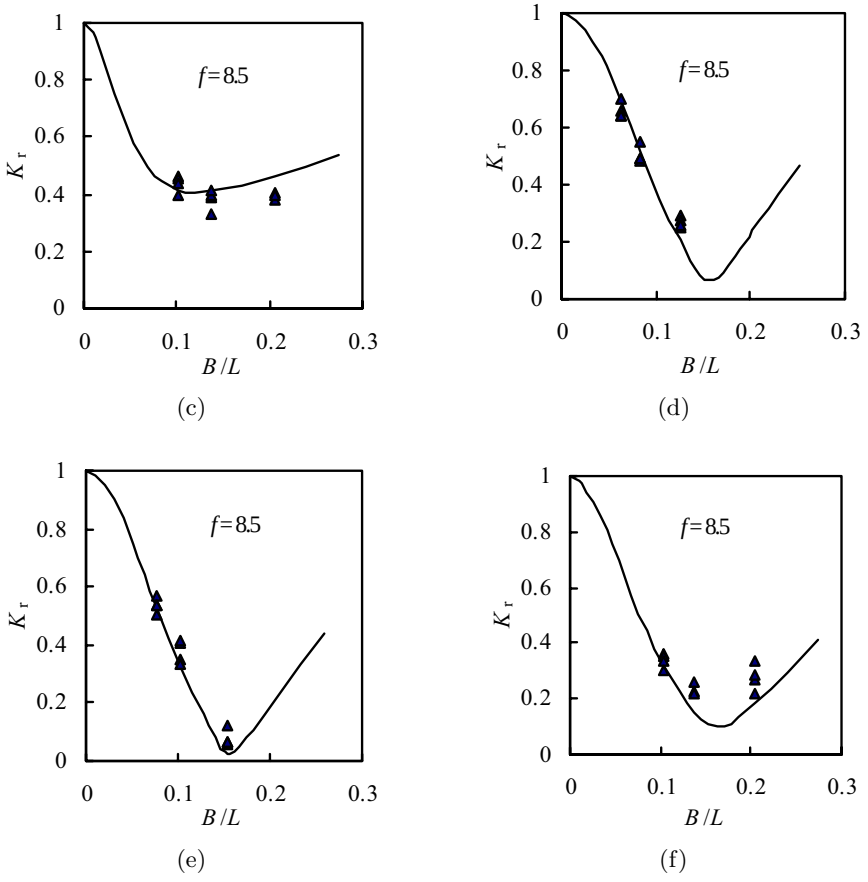

Fig. 15 (*Continued*)

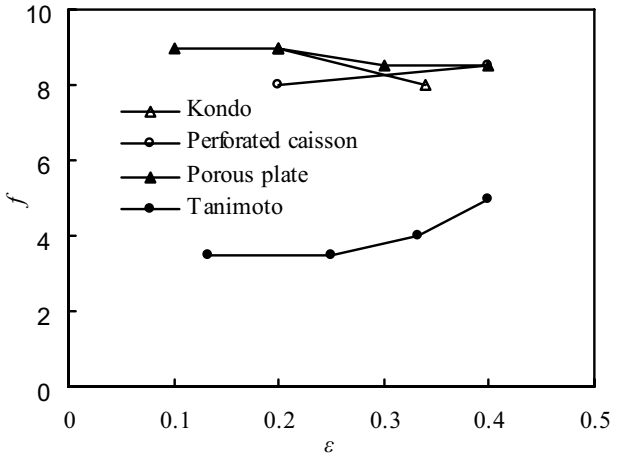

Fig. 16. Influence of porosity ε on f.

Table 4. Values of f at different conditions.

Experiments	Relative plate thickness b/d	Values of f							
		$\varepsilon = 0.1$	0.133	0.2	0.25	0.3	0.34	0.4	0.58
Zhu [2001a]	0.0094			9.5					
Kondo [1979]	0.012			9			8		
Perforated caisson	0.025			8				8.5	
Porous plate	0.0286	9		9		8.5		8.5	
Twu [1991]	0.048								5.5
Tanimoto [1982]	0.05		3.5		3.5		4	5	
	0.1, 0.15				2				

of $s = 1$ is also recommended for thin permeable plate. All the results are listed in Table 4.

For a given plate, a constant f value has been used for predicting the reflection and transmission coefficients in the above comparisons. In general, the agreements between predicted and experimental results are reasonably good. It also can be seen from the comparisons with Tanimoto and Yoshimoto [1982] that, for a special porous plate with a constant porosity of 0.25 (Fig. 4), the reflection coefficients for different water depth d_1 in the chamber can all be well predicted with a constant value of f ($f = 3.5$). Therefore, it can be concluded that, for a given plate, the value of f is much insensitive to the wave factors based on the Airy wave theory. Actually, Li *et al.* [2002, 2003b] also concluded that the wave height has little influence on the coefficients of wave reflection and transmission for a porous plate. Losada *et al.* [1993] also described "The friction coefficient is independent of the flow and is associated with the porous structure. It can be determined experimentally for each structural configuration". In addition, the present porous plate experiment shows that the porous shapes have no obvious influence on the values of f as shown in Figs. 12(b), (e) and (f). This may be explained as follows. The permeable plate is assumed to be a rigid homogeneous porous medium. Thus, the different porous shapes may represent different pore shapes and arrangements in the porous medium. The study of Kondo [1979] suggested that the flow in a porous medium be turbulent in practices, and f be relatively independent of the Reynolds number. That is to say, the values of f are little related to the velocity and the pore shape (i.e. porous shape) in the porous medium (i.e. permeable plate).

The influence of porosity ε on the resistance coefficient f is shown in Fig. 16. It can be seen that the f increases with the increase of ε in Tanimoto and Yoshimoto's [1982] and present partially perforated caisson experiments. But the trend is opposite in the experiment of Kondo [1979] and present porous plate experiment. It does not seem easy to estimate the influence of porosity. However, it can be also found from Fig. 16 that the values of f vary only little with the increasing of porosity in the range of $\varepsilon = 0.1$–0.25, which are usually used in engineering. Isaacson *et al.* [1998,

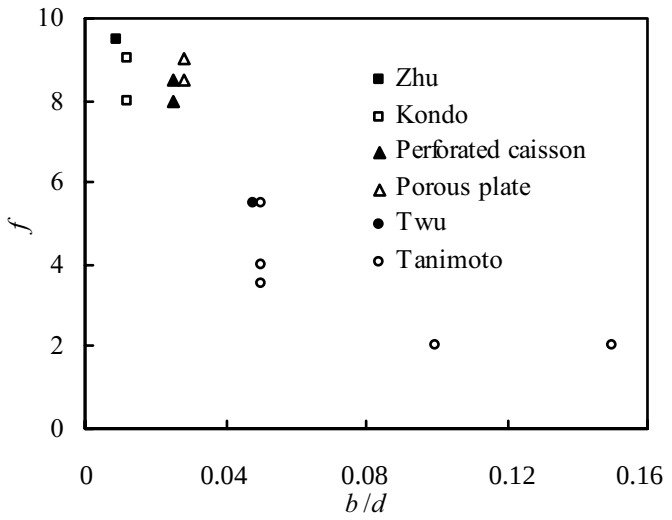

Fig. 17. Influence of b/d on f.

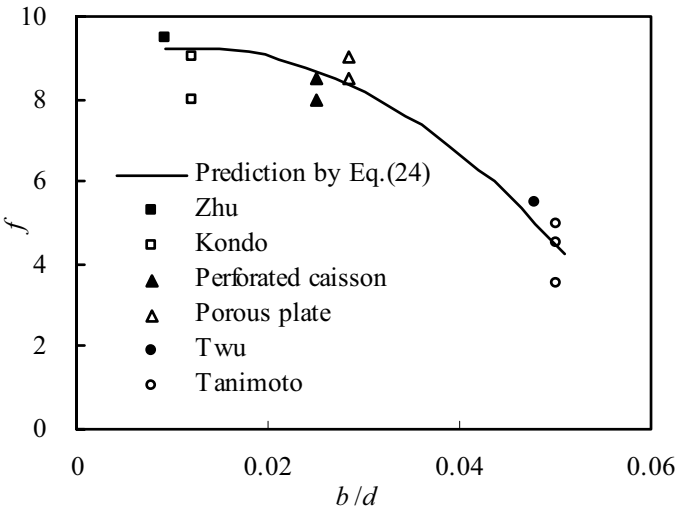

Fig. 18. Comparison of predicted f with experimental results as function of b/d.

1999] also suggested that f may not be sensitive to the porosity. So, to consider the engineering application condition, the influence of porosity ε on f can be neglected.

Leaving out the influence of porosity, Fig. 17 shows the influence of relative plate thickness b/d on f. The values of f decrease with the increasing of relative plate thickness when $b/d < 0.1$. But f tends to be a constant value 2.0 as the rubble structure [Yu, 1995] when $b/d \geq 0.1$, where it may not be much appropriate employing the thin plate hypothesis. A formula of f with b/d is obtained

using the least square method as follow:

$$f = -3338.7\left(\frac{b}{d}\right)^2 + 82.769\left(\frac{b}{d}\right) + 8.711 \quad 0.0094 \leq \frac{b}{d} \leq 0.05 \tag{24}$$

The correlation coefficient of Eq. (24) is 0.956, and the formula can be safely used in the range of $0.0094 \leq b/d \leq 0.05$. The values of f calculated with Eq. (24) agree well with that estimated from different experiments, as shown in Fig. 18.

The porous effect parameter G can be calculated by using Eqs. (22) and (24) when s is unit, and the results can be applied to engineering designs. In practice, engineers often give more attention to the wave loads on permeable structures. We will compare the values of G estimated using present method with the several G obtained by Li *et al.* [2002, 2003b], and use the G to calculate the total horizontal wave loads on the partially perforated caissons. The method employed by Li *et al.* [2002, 2003b] is as follows: the reflection and transmission coefficients of a porous plate with rectangular holes are measured, then, the values of G are reversely calculated by using Eqs. (2) and (3). The values of G with four different periods are given. The G given by Li *et al.* [2002, 2003b] and the corresponding G calculated with the present method are listed in Table 5. The corresponding wave factors and water depth are the same as the present perforated caisson experiment.

The total horizontal wave loads on the models of the present perforated caisson experiment are calculated using Eqs. (18)–(20) with two different G listed in Table 5, and the comparisons between them are shown in Fig. 19. The total horizontal wave loads on unit length are represented dimensionlessly as $F/\rho g H d$, where F is the wave loads on unit length, ρ the water density, g the gravitational acceleration, H the wave height and d the water depth. It can be seen from Table 5 that the G values by two ways are close. As a result, the calculated results of wave loads are also quite close as shown in Fig. 19. The comparison of the total horizontal wave loads between the predictions with present G and the experimental results is shown in Fig. 20, where the two dashed lines represent $y = (1 \pm 10\%)x$, respectively. The agreement of predicted values and experimental results is satisfying. This indicates that satisfying numerical wave load results can be obtained by using the present complete estimate method of the porous effect parameter G.

Table 5. G obtained by Li *et al.* [2002, 2003b] and present method ($b/d = 0.025$).

Incident wave period (s)	Porous effect parameter G			
	Li *et al.* $\varepsilon = 0.2$	Present $\varepsilon = 0.2$	Li *et al.* $\varepsilon = 0.4$	Present $\varepsilon = 0.4$
1.4	0.79 + 0.05i	0.86 + 0.09i	1.88 + 0.51i	1.73 + 0.20i
1.2	0.69 + 0.00i	0.70 + 0.08i	1.85 + 0.00i	1.40 + 0.16i
1.0	0.68 + 0.00i	0.53 + 0.06i	1.09 + 0.00i	1.06 + 0.12i
0.86	0.65 + 0.00i	0.41 + 0.05i	0.85 + 0.00i	0.81 + 0.09i

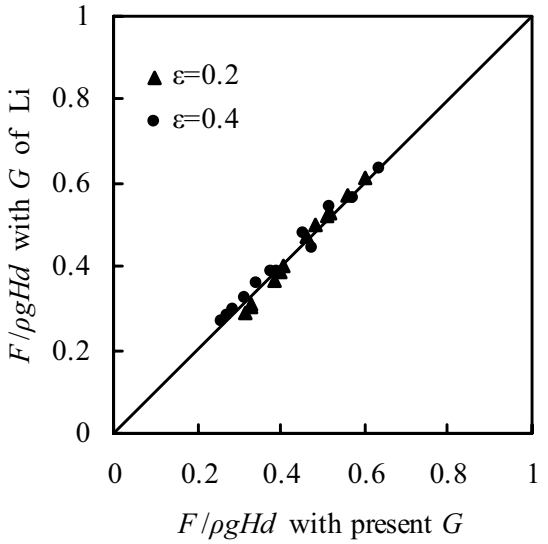

Fig. 19. Comparison of predicted horizontal wave loads with different G of present and Li *et al.* [2002, 2003b].

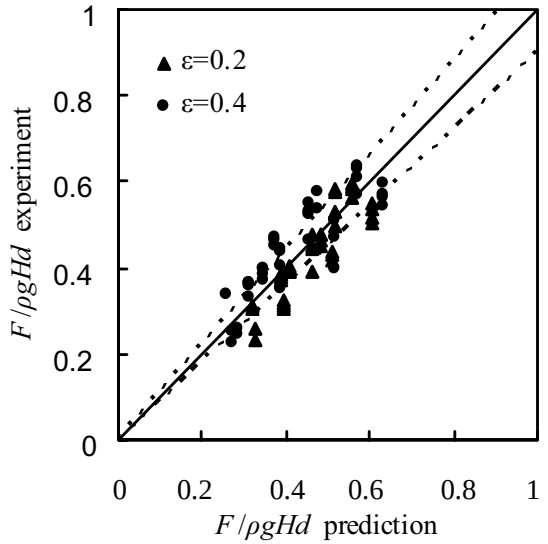

Fig. 20. Comparison of predicted values of horizontal wave loads with experimental results.

5. Conclusions

In the present study, the analytical solutions of wave interactions with two typical permeable breakwaters are introduced based on the Airy wave theory. A complete estimate method of the porous effect parameter G is developed by comparing the predicted values of the reflection and transmission coefficients with the experimental data. The estimate method consists of Eqs. (22) and (24) with $s = 1$. The G values

are used for calculating the horizontal wave loads on partially perforated caissons. The agreement of calculating results and experimental data is satisfying, which validates the developed method by the authors.

Some phenomena are found in our analysis as follows. The resistance coefficient f is not sensitive to the porous shape and porosity. The f is independent of the flow and is associated with the porous plate itself. The relative plate thickness b/d is the main effect parameter of f. The f increases with the decreasing of b/d. But when $b/d \geq 0.1$, f can be treated as 2.0.

The present paper gives entirely the calculating methods of horizontal wave loads and reflection coefficients of permeable wall structures. It can be used as a theoretical base for engineering application.

Acknowledgments

This study is financially sponsored by the Program for Changjiang Scholars and Innovative Research Team in University (Project No. IRT0420), and the foundation for the development of design specification by the Ministry of Communication, China. Special thanks are due to Prof. Allen T. Chwang and Dr. S. T. Zhu for their offering experimental information to the authors. Prof. H. Kojima, Dr. T. Sakakiyama and an anonymous reviewer are sincerely acknowledged for their helpful comments.

Appendix A

Assuming the thin plate (region Ω_3) as a rigid homogenous porous medium, the flow control equations are as follows [Sollit and Cross, 1972]:

$$\nabla \cdot U = 0 \tag{A.1}$$

$$s\frac{\partial U}{\partial t} = -\frac{\nabla P}{\rho} - f\omega U \tag{A.2}$$

in which,

$$s = 1 + C_m \frac{1-\varepsilon}{\varepsilon} \tag{A.3}$$

where U = fluid velocity, ρ = water density, P = water pressure, ω = angular frequency, f = linearized resistance coefficient, s = inertial effect coefficient, C_m = added mass coefficient and ε = porosity. Considering harmonic solutions, the time factor $e^{-\mathrm{i}\omega t}$ of U and P can be extracted out as follows: $U = \mathrm{Re}[\mathrm{u}\, e^{-\mathrm{i}\omega t}]$ and $P = \mathrm{Re}[pe^{-\mathrm{i}\omega t}]$. The spatial functions $\mathbf{u}$ and p satisfy the following equations:

$$\nabla \cdot \mathrm{u} = 0 \tag{A.4}$$

$$\mathrm{u} = \frac{\nabla p}{\rho}\frac{1}{\omega(f - \mathrm{i}s)} \tag{A.5}$$

It can be found by nondimensionalizing Eqs. (A.4) and (A.5) that the gradients of the velocity and pressure in the x-direction are predominant. Thus, only the horizontal velocity component should be considered, and a linear correction between velocity component in the x-direction and pressure difference in the plate can be developed:

$$u = \frac{1}{\rho b \omega (f - \mathrm{i}s)} (p_0^+ - p_b^-) \tag{A.6}$$

where u = velocity component in the x-direction, symbols $^+_0$ and ^-_b represent the values at $x = 0$ and $x = b$ in the porous plate, $^-_0$ and ^+_b represent the values at $x = 0$ and $x = b$ outside the porous plate. Considering $p_0^+ = p_0^-$ and $p_b^+ = p_b^-$, and matching the fluid velocities in and outside the plate, then,

$$u_0^- = u_b^+ = \varepsilon u = \frac{\varepsilon}{\rho b \omega (f - \mathrm{i}s)} (p_0^- - p_b^+) \tag{A.7}$$

Pressure p_0^- and p_b^+ and spatial potential ϕ_1 and ϕ_2 satisfy the linear Bernoulli Equations: $p_0^- = \mathrm{i}\omega\rho\phi_1$ and $p_b^+ = \mathrm{i}\omega\rho\phi_2$. Neglecting the plate thickness b, we can get $\partial\phi_1/\partial x = u_0^- = u_b^+ = u_0^+ = \partial\phi_2/\partial x$, and a porous boundary condition can be developed:

$$\frac{\partial\phi_1}{\partial x} = \frac{\partial\phi_2}{\partial x} = \mathrm{i}k_0 G(\phi_1 - \phi_2) \quad x = 0^{\pm} \tag{A.8}$$

in which,

$$G = \frac{\varepsilon}{k_0 b (f - \mathrm{i}s)} = G_r + \mathrm{i}G_i \tag{A.9}$$

where G is the porous effect parameter, k_0 is the incident wave number and satisfies the dispersion equation $\omega^2 = gk_0 \tanh k_0 d$.

References

Bennett, G. S., McIver, P. & Smallman, J. V. [1992] "A mathematical model of a slotted wavescreen breakwater," *Coastal Eng.* **18**, 231–249.

Chen, K. H., Chen, J. T., Lin, S. Y. & Lee, Y. T. [2004] "Dual boundary element analysis of normal incident wave passing a thin submerged breakwater with rigid, absorbing, and permeable boundaries," *J. Waterway, Port, Coastal, and Ocean Eng., ASCE* **130**(4), 179–190.

Chwang, A. T. [1983] "A porous-wavemaker theory," *J. Fluid Mech.* **132**, 395–406.

Goda, Y. & Suzuki, Y. [1976] "Estimation of incident and reflected waves in random wave experiments," *Proc. 15th Coast. Eng. Conf., ASCE*, pp. 828–845.

Hossain, A., Kioka, W. & Kitano, T. [2001] "Transmission of long waves induced by short-wave groups through a composite breakwater," *Coastal Eng. J.* **43**(2), 83–97.

Isaacson, M., Baldwin, J., Premasiri, S. & Yang, G. [1999] "Wave interactions with double slotted barriers," *Applied Ocean Research* **21**, 81–91.

Isaacson, M., Premasiri, S. & Yang, G. [1998] "Wave interactions with vertical slotted barrier," *J. Waterway, Port, Coastal, and Ocean Eng., ASCE* **124**(3), 118–126.

Jarlan, G. E. [1961] "A perforated vertical wall breakwater," *The Dock and Harbour Authority* **XII**(486), 394–398.

Kondo, H. [1979] "Analysis of breakwaters having two porous walls," *Coastal Structures'79, ASCE*, Alexandria, VA, pp. 962–977.

Li, Y. C., Dong, G. H., Liu, H. J. & Sun, D. P. [2003a] "The reflection of oblique incident waves by breakwaters with double-layered perforated wall," *Coastal Eng.* **50**, 47–60.

Li, Y. C., Liu, H. J., Teng, B. & Sun, D. P. [2002] "Reflection of oblique incident waves by breakwaters with partially-perforated wall," *China Ocean Eng.* **16**(3), 329–342.

Li, Y. C., Sun, L. & Teng, B. [2003b] "Wave action on double-cylinder structure with perforated outer wall," *OMAE'03*, Vol. 1, pp. 149–156.

Losada, I. J., Losada, M. A. & Baquerize, A. [1993] "An analytical method to evaluate the efficiency of porous screens as wave dampers," *Applied Ocean Research.* **15**, 207–215.

McIver, P. [1999] "Water-wave diffraction by thin porous breakwater," *J. Waterway, Port, Coastal, and Ocean Eng., ASCE* **125**(2), 66–70.

Mei, C. C., Liu, P. L.-F. & Ippen, A. T. [1974] "Quadratic loss and scattering of long waves," *J. Waterways, Harbors and Coastal Eng. Division* **100**(WW3), 217–239.

Requejo, S., Vidal, C. & Losada, I. J. [2002] "Modelling of wave loads and hydraulic performance of vertical permeable structures," *Coastal Eng.* **46**, 249–276.

Sahoo, T., Lee, M. M. & Chwang, A. T. [2000] "Trapping and generation of waves by vertical porous structures," *J. Eng. Mech.* **126**(10), 1074–1082.

Sollit, C. K. & Cross, R. H. [1972] "Wave transmission through porous breakwaters," *Proc. 13th Coastal Eng. Conf., ASCE*, Vancouver, pp. 1827–1846.

Tanimoto, K. & Yoshimoto, Y. [1982] "Theoretical and experimental study of reflection coefficient for wave dissipating caisson with a permeable front wall," *Report of the Port and Harbour Research Institute* **21**(3), 44–77 (in Japanese, with English abstract).

Teng, B., Zhang, X. T. & Ning, D. Z. [2004] "Interaction of oblique waves with infinite number of perforated caissons," *Ocean Eng.* **31**, 615–632.

Twu, S. W. & Liu, C. C. [2004] "Interaction of non-breaking regular waves with a periodic array of artificial porous bars," *Coastal Eng.* **15**, 223–236.

Twu, S. W. & Lin, D. T. [1991] "On a highly effective wave absorber," *Coastal Eng.* **15**, 389–405.

van Gent, M. R. A. [1995] *Wave Interaction With Permeable Coastal Structures*, PhD Thesis, Delft University of Technology, pp, 22–46.

Yu, X. [1995] "Diffraction of water waves by porous breakwaters," *J. Waterway, Port, Coastal, and Ocean Eng., ASCE* **121**(6), 275–282.

Zhao, M. & Teng, B. [2004] "A composite numerical model for wave diffraction in a harbor with varying water depth," *Acta Oceanologica Sinica* **23**(2), 367–375.

Zhu, S. & Chwang, A. T. [2001a] "Investigation on the reflection behaviour of a slotted seawall," *Coastal Eng.* **43**, 93–104.

Zhu, S. & Chwang, A. T. [2001b] "Analytical study of porous wave absorber," *J. Eng. Mech.* **127**(4), 326–332.